



Mariana Petronela Hanga ORCID iD: 0000-0002-2427-4052

Bioprocess development for scalable production of cultivated meat

Mariana Petronela Hanga^{1*}, Junaid Ali¹, Panagiota Moutsatsou¹, Fritz Anthony de la Raga¹, Christopher J Hewitt^{1†}, Alvin Nienow^{1,2}, Ivan Wall¹

1 – Department of Biosciences, School of Life and Health Sciences, Aston University, Aston Triangle, Birmingham, United Kingdom

2 – Department of Chemical Engineering, University of Birmingham, Edgbaston, Birmingham, United Kingdom

[†]In memoriam of Prof Christopher J Hewitt who sadly passed away on 25th of July 2019

***Correspondence:** Dr Mariana Petronela Hanga, School of Life and Health Sciences, Aston University, Aston Triangle, Birmingham, B4 7ET, United Kingdom

E-mail: m.hanga@aston.ac.uk

Abstract

Traditional farm-based products based on livestock are one of the main contributors to greenhouse gas emissions. Cultivated meat is an alternative which mimics animal meat, being produced in a bioreactor under controlled conditions rather than through slaughtering of animals. The first step in the production of cultivated meat is the

This article has been accepted for publication and undergone full peer review but has not been through the copyediting, typesetting, pagination and proofreading process, which may lead to differences between this version and the Version of Record. Please cite this article as doi: 10.1002/bit.27469.

This article is protected by copyright. All rights reserved.

Accepted Article

generation of sufficient reserves of starting cells. In this study, bovine adipose-derived stem cells (bASCs) were used as starting cells due to their ability to differentiate towards both fat and muscle, two cell types found in meat. A bioprocess for the expansion of these cells on microcarriers in spinner flasks was developed. Different cell seeding densities (1,500, 3,000 and 6,000 cells/cm²) and feeding strategies (80%, 65%, 50% and combined 80/50% medium exchanges) were investigated. Cell characterisation was assessed pre- and post-bioprocessing to ensure that bioprocessing did not negatively affect bASC quality. The best growth was obtained with the lowest cell seeding density (1,500 cells/cm²) with an 80% medium exchange performed ($p < 0.0001$) which yielded a 28-fold expansion. The ability to differentiate towards adipogenic, osteogenic and chondrogenic lineages was retained post-bioprocessing and no significant difference ($p > 0.5$) was found in clonogenicity pre- or post-bioprocessing in any of the feeding regimes tested.

Keywords: cultivated meat, bovine adipose-derived stem cells (bASCs), bioprocessing, microcarriers, spinner flasks

1. Introduction

There is an increased need for sustainable, protein rich food sources to support the rapidly growing population (Arshad *et al*, 2017). There is also a direct correlation between increasing per capita income and meat consumption (Stephens *et al*, 2018; Gerbens-Leenes *et al*, 2010), so that developing countries are expected to significantly impact the global demand for meat products. The food and agriculture organisation of the United Nations (FAO) report from 2016 predicts an increase of 48 Mega tons for meat demand by 2025 with 73% of this increase coming from developing countries such as Brazil and China (OECD/FAO, 2016). With animal agriculture currently

occupying 70% of arable land, generating 14.5% of anthropogenic greenhouse emissions (Grossi *et al*, 2019) and consuming 27% of fresh water resources just for livestock feed production (Gerbens-Leenes *et al*, 2013), it becomes evident that conventional animal agriculture and meat production methods cannot sustain such growth in meat demand. Alternative food technologies such as cultivated meat might provide a solution to this growing problem (Salonen & Helne, 2012; Fan *et al*, 2019; Stephens *et al*, 2018), as initial projections show that it will require 45% less energy, 99% less land and will emit 78-96% less greenhouse gas emissions (Tuomisto *et al.*, 2011; Stephens *et al*, 2018). Other life cycle analyses of cultured meat production showed that the environmental impact is highly dependent on the type of meat produced (Mattick *et al*, 2015), as well as the method of energy production employed in the manufacturing (Smetana *et al*, 2015). As the production of cultivated meat will most likely require the use of bioreactors to achieve the necessary scale, the energy requirement for operation of bioreactors could have a significant environmental impact. However this problem could be minimised in the future if decarbonisation of energy production can be achieved (Bodiou *et al*, 2020). Cultivated meat can undoubtedly have a positive impact on animal welfare and can also offer a potentially healthier and safer option for consumers as the production process can be closely controlled and possibly tuned to produce meat that is free from antibiotics, free from zoonotic bacteria and viruses and with a specific, desired nutritional profile (*e.g.* enriched in omega fatty acids, reduced cholesterol).

In 2013, the worlds' first cultivated meat burger was produced by Prof Mark Post as a proof of concept, however with a cost of approximately £250,000 (Mouat & Prince, 2018). In the past couple of years, the interest in cultivated meat and its potential benefits has increased significantly. Now there is a race to bring commercially viable

cultivated meat products to the market, but to achieve this, research to increase product output *i.e.* yield and to decrease cost must be conducted. The underpinning biological knowledge needed to produce a cultivated meat product is somewhat understood. The first step in cultivated meat production is the choice of the starting cell source. Some research groups in the field of cultivated beef use bovine satellite cells which are dedicated muscle progenitors (Verbruggen *et al.*, 2017; Katim *et al.*, 2015). However, these cells can only differentiate towards muscle. Meat is complex and comprises several types of tissues (*e.g.* muscle, fat, connective tissue) (Listrat *et al.*, 2016), thus using satellite cells as starting material is not sufficient as it requires the addition of other cell types (*e.g.* fat) from other sources. Mesenchymal stem cells on the other hand, have the ability to differentiate towards both adipogenic and myogenic lineages (Okamura *et al.*, 2018; Bosnakovski *et al.*, 2005), thus being able to produce both cell types of interest (*e.g.* muscle and fat) for production of cultivated meat. Additionally, mesenchymal stem cells are easy to isolate from a variety of tissues such as bone marrow, adipose, umbilical cord, placenta and foetal fluids (Hill *et al.*, 2019). In this study, bovine adipose-derived stem cells (bASCs) were chosen as a starting cell source.

The first step in the production of cultivated meat is the expansion phase, *i.e.* the production of quality starting cells. It has been estimated that the number of cells required for producing 1 kg of protein from muscle cells will be of the order of 2.9×10^{11} cells (Allan *et al.*, 2019)) to 8×10^{12} cells (Stephens *et al.*, 2018). Such cell numbers are in any realistic sense unattainable from monolayer culture, but microcarriers used in conjunction with stirred bioreactors are a much more feasible option. For example, one 5L stirred bioreactor with a 5000 cm² surface area provided by microcarriers per litre was able to produce as many human MSCs as 65 T-flasks at confluence (Rafiq *et al.*, 2013). To date, there are many other published studies focused

on the use of stirred bioreactors for the expansion of human MSCs at different scales (Hewitt *et al.*, 2011; Rafiq *et al.*, 2013; Heathman *et al.*, 2015; Rafiq *et al.*, 2017; deSoure *et al.*, 2016; Rafiq *et al.*, 2018; Lawson *et al.*, 2017). However, there is no available literature on the development of bioprocesses in stirred bioreactors for the expansion of bovine analogues.

Before moving to the litre scale bioreactors, due to cost considerations, process development for MSCs is typically carried out in spinner flasks which are essentially small stirred tank bioreactor vessels operated at the 100 to 250 mL scale (Hewitt *et al.*, 2011; Bardy *et al.*, 2013; Goh *et al.*, 2013; Schirmaier *et al.*, 2014). Spinner flasks are easy to use, provide a dynamic environment and are relatively-easily translatable to litre scale stirred tank bioreactors (Rafiq *et al.*, 2013). This manuscript focuses on the development of a scalable bioprocess in spinner flasks for the expansion of bASC as the first step in cultivated beef production. The objectives of this work were: 1) to establish bASCs cultures examining growth and cell product quality attributes; 2) to develop a scalable bioprocess in spinner flasks for bASCs expansion 3) to investigate if cell quality is retained post-bioprocessing.

2. Materials and methods

2.1 Planar culture of bovine adipose derived stem cells (bASC)

Bovine adipose derived stem cells (bASCs) were purchased from Cellider Biotech (Spain) and stored in liquid nitrogen. Upon thawing, the cells were cultured in T-flasks using a growth medium comprising of α -Modified Eagle Medium (1 g/L glucose, Lonza, UK) supplemented with 10% (v/v) foetal bovine serum (FBS; Sigma Aldrich, UK), 1 ng/mL bFGF (Peprotech, UK) and 2mM ultraglutamine (Lonza, UK). bASCs

between passage numbers 2 and 10 were used for the planar study, while for the microcarrier cultures, only cells between passage numbers 2 and 5 were used. The cells were stored in a humidified incubator, at 37°C and 5% CO₂. A complete medium exchange was performed after 72 hours in culture and cells were passaged at day 5 when ~80% confluency was achieved. Cell passage was performed with 0.25% trypsin-EDTA (Gibco, Thermofisher, UK) for 8 minutes at 37°C until complete cell detachment. The enzyme was then inactivated by the addition of growth medium and the cell suspension was centrifuged at 250g for 5 minutes.

2.2. Microcarrier culture in spinner flasks

The inside of the spinner flasks (100 mL working volume with a magnetic rod impeller equipped with a paddle (Figure 3A), Belco (US)) were first coated with Sigmacote (Sigma Aldrich) to prevent cells attaching to their inner surface. Plastic microcarriers (Pall, UK) were weighed to achieve a surface area of 5 cm²/mL in the spinner, which were then sterilised by autoclaving. bASCs between passage numbers 2 and 5 were seeded at different seeding densities of 1,500, 3,000 and 6,000 cells/cm² of microcarrier surface. Upon seeding, the spinner flasks were stored in a humidified incubator at 37°C and 5% CO₂. Different feeding regimes ranging from 50% to 80% medium exchanges were investigated with the first carried out at day 3 and then every other day. Samples were taken regularly during culture to enable cell imaging, cell counts and analysis for glucose and lactate. The spinner flask cultures were agitated at the minimum speed required for microcarrier suspension, N_{js} (30 rpm) for the first 3 days (Hewitt *et al*, 2011; Nienow *et al.*, 2016a), followed by an incremental increase of 10 rpm every 2 days thereafter to ensure suspension was maintained and to control aggregation of microcarriers, as cells on them were growing more confluent. The cultures were kept

for up to 9 days when full harvest was performed by using a previously described protocol (Nienow *et al.*, 2016b). Briefly, two washes with DPBS were performed while stirring, followed by incubation with 0.25% trypsin-EDTA at 37°C while stirring at 150 rpm for 10 minutes. During the last 10 seconds of incubation, the agitation was increased to 250 rpm. The aim of this approach was to use the high specific energy dissipation rate to enhance the detachment of the cells from the microcarriers. The advantage of this period of high agitation intensity is that essentially 100% of the cells are detached from the microcarriers and the time during which potential damage to the cells could occur from the detachment enzyme is greatly reduced. In addition, as soon as the cells are detached, they are smaller than the microscale of turbulence and the cells do not get damaged by fluid dynamic stresses (Nienow *et al.*, 2016a; Nienow *et al.*, 2016b). Once the cells were completely detached from the microcarriers, the cell-microcarrier suspension was passed through an 80 µm filter (Steriflip), which removed the microcarriers and the cell suspension was then centrifuged at 250g for 5 minutes.

2.3. Cell characterisation

2.3.1. Tri-lineage differentiation potential

All chemicals were purchased from Sigma Aldrich unless otherwise stated. SCs were differentiated towards adipogenic, osteogenic and chondrogenic lineages using StemPro differentiation kits (Thermofisher). A 12-well plate was used for all experiments. bASCs were seeded at 5,000 cells/cm² for osteogenic differentiation and 10,000 cells/cm² for adipogenic differentiation. For chondrogenic differentiation, the macromass method was used (Heathman *et al.*, 2015). Briefly, 5 µL droplets of a highly concentrated bASCs suspension (1x10⁷ cells/mL) were seeded in an empty well plate and allowed to attach for 1-2 h at 37°C in a CO₂ incubator. Upon cell attachment,

chondrogenic differentiation medium (Stempro) was added. For all differentiation cultures, the cells were grown in their respective media for 21 days with a medium change performed every 3-4 days. At the end of 21 days, the cells were fixed with 4% paraformaldehyde for 20 minutes at room temperature. Adipogenic differentiation was assessed by using LipidTox green (Thermofisher) to stain lipid vesicles in adipogenic differentiated cells. The stain was used according to the manufacturer's instructions. Osteogenic differentiation potential was assessed using von Kossa stain as previously described (Hanga *et al*, 2017). Silver nitrate was used to stain bone mineralisation, while also assessing alkaline phosphatase expression. Chondrogenic differentiation was assessed by Alcian blue staining (Hanga *et al*, 2017).

2.3.2. Clonogenicity

Three hundred cells were seeded into a T-25 flask in growth medium and placed into an incubator set to 37°C and 5% CO₂. The medium was changed every 3-4 days and the flasks were kept for up to 14 days. The medium was then removed and cells were fixed and stained with 1% crystal violet (Sigma Aldrich, UK) for 30 minutes at room temperature. The stained colonies were then manually counted.

2.3.3. Cell surface marker expression

Immunofluorescence staining was performed to assess expression of a panel of three cell surface markers identified as indicative of mesenchymal stem cells and these were: CD73 (Abcam), CD90 (Abcam) and CD105 (Thermofisher). Cells were fixed using 4% para-formaldehyde for 20 minutes at room temperature and then permeabilised using Perm Wash 1X (Biolegend) for 5 minutes. Cells were then incubated with 10% normal goat serum (Thermofisher) for 45 minutes in the dark to block any non-specific binding, followed by incubation overnight at 4°C with the primary antibody at the recommended

dilution and then incubation for 2h at room temperature with the secondary antibody at the manufacturer's recommended dilution. DAPI was used for staining the nuclei and Phalloidin (Sigma Aldrich) was used to stain the cytoskeleton. Cells were then visualised and imaged under a fluorescence microscope (Evos FL Thermofisher).

2.4. Analytical techniques

Imaging was performed by either phase contrast microscopy or fluorescence microscopy. Live/dead staining (Calcein AM/ Ethidium Homodimer) kit (Thermofisher) was used to assess cell viability on microcarriers following manufacturer's instructions. Cell counts were performed using the NucleoCounter NC-3000 (Chemometec). For the spinner flasks cultures, cell counts were performed directly onto microcarriers using the reagent A100 and reagent B protocol. Briefly, the cell-microcarrier suspension was diluted in a 1:3 ratio with reagent A100 (lysing agent) and then reagent B (stabilizing agent). The resulting suspension was then loaded onto a Nucleocassette that contains acridine orange and DAPI. Spent medium samples were collected before and after medium exchanges and analysed for glucose and lactate concentrations on a Roche AccuTrend Plus meter. Fresh growth medium was used as baseline control. Based on cell counts, the following parameters were calculated:

1. Specific growth rate

$$\mu = \frac{\ln(Cx(t)/Cx(0))}{\Delta t} \text{ [eq. 1]},$$

2. Doubling time

$$t_d = \frac{\ln 2}{\mu} \text{ [eq. 2]},$$

3. Fold increase

$$FI = \frac{Cx(t)}{Cx(0)} \text{ [eq. 3]},$$

4. Cumulative population doublings

$$CPDL = \Sigma \left[\frac{1}{\log 2} * LOG \left(\frac{Cx(t)}{Cx(0)} \right) \right] \text{ [eq. 4]},$$

where μ is the specific growth rate (h^{-1}); t_d is doubling time (h); FI is fold increase; CPDL is cumulative population doublings; $Cx(t)$ and $Cx(0)$ represent cell numbers at the end and start of the culture; t represents time in culture (h).

2.5. Statistical analysis

All experiments were performed in triplicates with primary cells from the same animal. Cell counts were acquired from two independent samples from each replicate. Data was expressed as mean \pm SD. Statistical analysis was carried out using Graph Pad Prism 8. For comparison between two data sets, statistical significance was determined by Student's two-tailed t-test. For comparison of multiple data sets, significance was calculated by one-way ANOVA. Significance was determined at $p < 0.05$.

3. Results and discussion

3.1. Establishing a baseline for bASCs expansion

The first step was to establish a baseline for growth and quality of the bASCs. For this, the cells were cultured for 10 consecutive passages. bASCs morphology was monitored throughout the entire duration of the continued culture and it was found to be fibroblast-like and similar to that reported for human mesenchymal stem cells (hMSCs) (Heathman *et al*, 2016) (Figure 1A). In comparison to hMSCs, bASCs were found to

be smaller with sizes ranging from 13 μ m at the earlier passages to 16 μ m at the later passages (*Figure 1C*). An increase in cell size for mesenchymal stem cells is usually associated with senescence and slowdown of growth (Wagner *et al*, 2008) which was also found applicable to bASCs. Passage 2 cells had a doubling time of 42.32 \pm 0.83 h at a cumulative population doubling of 5.99 \pm 0.06, while passage 8 cells were found to have a doubling time of 199.55 \pm 30.16 h at a cumulative population doubling of 20.67 \pm 0.09. Beyond passage 8 (at approximately 20 population doublings), cell growth slowed down (*Figure 1B*). Knowing this profile is important as it dictates the flexibility in handling bovine cells before senescence is reached and cells become old and unusable. This information also shows what range of cell passages can be used for bioreactor inoculation to avoid reaching senescence. Guidelines for hMSCs characterisation were previously published by Dominici *et al* (2006); however no such quality guidelines have been set for their bovine analogues. As a result, the same Dominici guidelines were used here. The quality baseline for bASCs was assessed through differentiation towards the three lineages (adipogenic, osteogenic, chondrogenic), expression of cell surface markers (CD90, CD73 and CD105) and clonogenicity potential. Human MSCs have positive expression of markers such as CD73, CD90 and CD105 and lack expression of markers such as CD34, CD45, HLA-DR, CD14, CD11b and CD19. Previous studies have shown that bovine mesenchymal stem cells have positive expression of some of the same markers as their human analogues (*e.g.* CD73, CD90 and CD105), but they also express additional markers such as CD29, CD166, CD44 and do not express CD45 or CD34 (Hill *et al*, 2019; Gao *et.al*, 2014). Here, the expression of CD73, CD90 and CD105 (*Figures 1D, 1E and 1F*) was assessed and was found to be positive.

Differentiation to osteogenic lineage was deemed successful as bone mineralisation was visibly stained in black, while alkaline phosphatase expression which is specific to osteocytes (van der Plas *et al*, 1994) was evident through the red staining (*Figure 2B*). Similarly, chondrogenic differentiation was also deemed successful as macromasses were formed and stained in blue (*Figure 2C*) indicating strong formation of GAGs representative to cartilage (Kuiper and Sharma, 2015). However, adipogenic differentiation was limited as indicated by the limited green fluorescence shown in *Figure 2A* indicating lipid vesicles typically present in adipocytes. The adipogenic differentiation efficiency (calculated as % of cells presenting lipid droplets per total number of cells) was found to be 12.1% \pm 2.8 (n=1982 cells analysed). This limited differentiation efficiency could be a direct result of the formulation of differentiation medium used here which was the commercially available Stempro (Thermofisher). As stem cells have an increased potential to cure diseases, their applicability is highly popular in human cell therapies (Watt *et al*, 2010). As a result, there is a huge market for reagents specifically formulated for human cells. Cultivated meat, on the other hand, is a newly developed concept that utilises stem cells from other species than human (*e.g.* bovine, porcine, ovine, poultry). Unfortunately, as this is a developing area, the availability of reagents specifically formulated for other species than human is limited. As the Stempro adipogenic differentiation medium is specifically formulated for human cells, the differences in the metabolism of bovine cells and human cells are not taken into consideration (Dodson *et al.*, 2010), thus explaining the limited differentiation potential of bASCs to adipogenic lineage. Clonogenicity potential was also assessed at an early passage (p2) and late passage (p7) (*Figure 2D*) and it was found to be significantly lower at the later passages (****p<0.0001).

3.2. Initial expansion of bASCs on microcarriers in spinner flasks

Microcarrier cultures were carried out in spinner flasks at the 100 mL scale (*Figure 3A*). The cells successfully attached to the microcarriers and by day 5, cell-microcarrier bridges were observed as indicated by white arrows in *Figure 3B* which is a sign of cell proliferation. Live/dead staining was used here to assess cell viability on the microcarriers, while also visualising the distribution of cells on their surface. *Figure 3C* shows an increased cell viability on microcarriers at day 5 with live cells stained in green and dead cells in red.

The initial microcarrier expansion was carried out at the same seeding density as in monolayer of 5,000 cells/cm² for 5 days. Cell growth on the microcarriers is compared to monolayer and is shown as fold increase in *Figure 4A*, specific growth rates in *Figure 4B* and doubling times in *Figure 4C*. No significant difference ($p > 0.05$) was found between cell growth in monolayer and on microcarriers. Similar fold increase values were obtained after 5 days of culture with 6.05 ± 0.31 in monolayer compared to 6.23 ± 1.69 in microcarrier culture. Similarly, a doubling time of $46.19 \text{ h} \pm 1.34$ was obtained in monolayer compared to $47.12 \text{ h} \pm 8.7$ in microcarrier culture. The similar growth on microcarriers was encouraging as this finding means that the bASCs can be expanded that way with its many advantages. These advantages include high surface area-to-volume ratio (provided that the microcarriers are adequately suspended, *i.e.* at not less than N_{JS} (Heathman *et al.*, 2018)) on which the cells can grow. It also facilitates the scalability of the bioprocess in other ways: a highly homogeneous environment leading to minimal gradients and the potential control of pH, temperature and concentration combined with enhanced oxygen transfer. These advantages minimise culture variability, reduce cell quality variation and lead to enhanced cost efficiency through

optimised feeding strategies thereby maximising cell growth, while minimising medium use.

3.3. Bioprocess enhancement for microcarrier expansion of bASCs in spinner flasks

Bioprocess improvement was initiated with studies of different cell seeding densities, which have previously been found to be important (Hewitt *et al.*, 2011) ranging from 1,500 cells/cm² to 6,000 cells/cm². The microcarrier cultures were carried out for up to 9 days. At the highest cell density (6,000 cells/cm²), the cell number increased exponentially up to day 5. However, beyond this time point, cell loss was observed (*Figure 5A*). This loss could be attributed to aggregation observed from day 5 onwards (*Figure 5B*) when most of the available surface area provided by the microcarriers was utilised leading to contact inhibition and arrest of cell growth (Eagle and Levine, 1967). At the intermediary cell seeding density tested (3,000 cells/cm²), a slight lag phase was observed until 72 h followed by a constant increase in cell number, while at the lowest seeding density of 1,500 cells/cm², no lag phase was observed (*Figure 5A*). At the highest cell seeding density (6,000 cells/cm²), glucose concentration constantly decreased up to day 5 in line with the increase in cell number, followed by an increase in concentration as the drop in cell number occurred. Related to these changes, the lactate concentration increased for the first 5 days, followed by a decrease thereafter (*Figure 5C*). At the lowest cell seeding density tested (1,500 cells/cm²), there was a sudden drop in glucose concentration to 2.47 mmol/L up to day 3 compared to 3.13 mmol/L obtained at the same time point for 6,000 cells/cm², followed by a subtle decrease until the end of the culture. During this time, the lactate concentration for this seeding density increased to 2.57 mmol/L at day 5 and remained constant thereafter (*Figure 5E*). These trends (*Figures 5C, 5D and 5E*) mirrored the cell growth profiles

for each cell seeding density tested (*Figure 5A*). It is also worth noting that in all of the growth conditions tested, inhibitory levels of lactate were not reached, *i.e.* >15 mM/L (Schop D. *et al*, 2009), so the slowdown in cell growth observed at the highest cell seeding density (6,000 cells/cm²) can only be attributed to confluency being reached on the microcarriers.

At the end of the culture, there was a consistent trend with the lowest cell seeding density of 1,500 cells/cm² generating a significantly higher fold increase of 28.8 ± 2.29 compared to 10.4 ± 3.39 for 3,000 cells/cm² and 5.08 ± 1.7 for 6,000 cells/cm² (**p<0.0001) (*Figure 6A*). Similarly, the lowest cell seeding density also generated a significantly higher specific growth rate (**p<0.0001) (*Figure 6B*) and a significantly lower doubling time (*p<0.05) (*Figure 6C*). A lower starting cell density is beneficial from a bioprocessing and handling point of view, as less 2D processing steps are required to get enough cells to seed a bioreactor culture, smaller cell banks can be used and more importantly, more doublings can be achieved in the same bioreactor size, allowing for less steps during the seeding train and therefore leading to lower production costs. Based on these results, the cell seeding density of 1,500 cells/cm² was selected for the next set of experiments investigating the impact of the feeding strategy.

In spinner flask cultures, 100% medium exchange is not possible if the aspiration of microcarriers is to be avoided leading to a loss of cells. In this study, 4 different medium exchange strategies were investigated ranging from 50% to 80% exchange throughout culture and a combination of 80% exchange for the first feeding point at day 3 followed by 50% exchange for the rest of the culture. For all investigated feeding strategies, medium exchanges were performed at day 3 and every other day thereafter. Additionally, the cell seeding density of 1,500 cells/cm² was used for all runs. The 80%

medium exchange yielded the highest cell number throughout culture (*Figure 7A*) with a fold increase of 28.01 ± 2.59 (**** $p < 0.0001$), while the 50% exchange yielded a fold increase of only 10.49 ± 2.95 . A doubling time of 45 ± 1.28 h was obtained when 80% exchange was performed, while a 50% exchange produced a doubling time of only 65.15 ± 7.15 h (*Table 1*). The glucose consumption and lactate production profiles for the different feeding strategies tested are shown in *Figures 7B, 7C, 7D and 7E*. When the 80% exchange was used, there was a continuous drop in glucose concentration and an increase in lactate concentration indicating good cell growth (*Figure 7B*). On the other hand, when a 50% exchange was used, the increase in lactate concentration was minimal to only 2.16 ± 0.055 mmol/L (*Figure 7E*) compared to 2.9 ± 0.17 mmol/L for 80% exchange at the end of the culture when the highest cell number was recorded. The glucose and lactate profiles showed a good correlation to the growth kinetics of bAMSCs at different exchange strategies.

It is well established that culture medium represents a large proportion of the manufacturing cost due to the large volumes needed when scaling up a bioprocess. Several strategies can be applied to reduce this cost and these include altering medium composition, recycling medium and some of its components or devising feeding strategies to minimise medium consumption and to maximise cell production (Van der Weele and Tramper, 2014; Stephens *et al*, 2018). The latter was investigated here. Thus, a cost analysis of consumables and reagents required for carrying out microcarrier culture in spinner flask at the working volume of 100 mL for 9 days was carried out. The main variable in this cost analysis was the volume of medium used as a result of different exchange strategies. The lowest cost found in relation to the cell number obtained was associated with the 80% medium exchange which was significantly lower (** $p < 0.001$) than the cost obtained for 50% medium exchange, but insignificant

compared to the 80/50% medium exchange where only the first medium exchange was 80% and the rest 50% (*Figure 8*). This analysis suggests that in the early stages of culture, nutrient availability and lack of metabolites are very important for cell growth.

3.4. Assessment of post-bioprocessing cell quality

It is important to acknowledge that exposure of the cells to the culture environment may have a detrimental effect on cell quality. As such, cell characterisation needs to be performed before and after bioprocessing to ensure that none of the steps taken during the bioprocess impacts negatively on the cell quality. Post-bioprocessing, the bASCs expanded in spinner flasks retained their ability to differentiate towards adipogenic, osteogenic and chondrogenic lineages (*Figures 8A, 8B and 8C*). Moreover, there was no significant difference ($p>0.5$) in the clonogenicity before and after bioprocessing at any of the feeding regimes tested (*Figure 8D*).

4. Conclusions

Meat is composed of several different types of cells (fat, muscle and connective cells). Bovine adipose-derived stem cells (bASCs) are a suitable cell source for production of cultivated meat as they have the ability to differentiate to both adipogenic and myogenic lineages. The first step in the production of cultivated meat is scalable expansion of starting cells. This study describes the development of a bioprocess in small stirred tank bioreactors (*e.g.* spinner flasks) for the expansion of bASCs. The best bioprocess developed included using a low cell seeding density of 1,500 cells/cm² of surface area, a feeding regime of 80% medium exchange and an agitation strategy of incremental increase every 2 days. These conditions yielded a 28-fold increase in cell number. The cells retained their cell surface marker expression and their ability to differentiate

towards adipogenic, osteogenic and chondrogenic lineages without any change in their clonogenicity. This bioprocess can serve as a starting point for translating the manufacturing of these bovine adipose-derived stem cells to the litre scale and beyond.

Acknowledgements

This work was made possible through funding received from The Good Food Institute, US through the 2018 GFI Competitive Grant Program.

Conflict of interest

The authors declare no financial or commercial conflict of interest.

References

Allan SJ, De Bank PA, Ellis MJ (2019) Bioprocess design considerations for cultured meat production with a focus on the expansion bioreactor. *Front Sustain Food Syst.*; 3:44. doi: 10.3389/fsufs.2019.00044

Arshad, M.S., Javed, M., Sohaib, M., Saeed, F., Imran, A. & Amjad, Z. (2017), Tissue engineering approaches to develop cultured meat from cells: A mini review, *Cogent Food & Agriculture*, 3(1):1320814. doi.org/10.1080/23311932.2017.1320814.

Bardy J, Chen AK, Lim YM, Wu S, Wei S, Weiping H, Chan K, Reuveny S, Oh SK. (2013). Microcarrier suspension cultures for high-density expansion and differentiation of human pluripotent stem cells to neural progenitor cells. *Tissue Eng Part C Methods*; 19(2):166-180. Doi: 10.1089/ten.TEC.2012.0146.

Bodiou V, Moutsatsou P, Post MJ (2020) Microcarriers for Upscaling Cultured Meat Production. *Front Nutr.*; 7:10. doi: 10.3389/fnut.2020.00010.

This article is protected by copyright. All rights reserved.

Bosnakovski D, Mizuno M, Kim G, Takagi S, Okumura M, Fujinaga T (2005) Isolation and multilineage differentiation of bovine bone marrow mesenchymal stem cells. *Cell Tissue Res*; 319(2), 243-253. DOI: 10.1007/s00441-004-1012-5.

Dodson MV, Hausman GJ, Guan L, Du M, Rasmussen TP, Poulos SP, Mir P, Bergen WG, Fernyhough ME, McFarland DC, Rhoads RP, Soret B, Reecy JM, Velleman SG, Jiang Z (2010) Lipid metabolism, adipocyte depot physiology and utilisation of meat animals as experimental models for metabolic research. *Int J Biol Sci*; 6(7), 691-699. DOI: 10.7150/ijbs.6.691.

Dominici M, Le Blanc K, Mueller I, Slaper-Cortenbach I, Marini F, Krause D, Deans R, Keating A, Prockop DJ, Horwitz E (2006) Minimal criteria for defining multipotent mesenchymal stromal cells. The International Society for Cellular Therapy position statement. *Cytotherapy*; 8(4), 315-317. DOI:10.1080/14653240600855905

Eagle H and Levine EM. (1967) Growth regulatory effects of cellular interaction. *Nature*, 213, 1102–1106. DOI: 10.1038/2131102a0

Fan A, Almanza B, Mattila AS, Ge L & Her E (2019) Are vegetarian customers more "green"?, *Journal of Foodservice Business Research*; 22(5), 467-482. Doi.org/10.1080/15378020.2019.1637221

Gao Y, Zhu Z, Zhao Y, Hua J, Ma Y, Guan W. (2014) Multilineage potential research of bovine amniotic fluid mesenchymal stem cells. *Int J Mol Sci.*; 15(3), 3698–3710. Doi: 10.3390/ijms15033698

Gerbens-Leenes PW, Nonhebel S, Krol MS (2010), Food consumption patterns and economic growth. Increasing affluence and the use of natural resources, *Appetite*, 55(3), 597-608. DOI: 10.1016/j.appet.2010.09.013.

Gerbens-Leenes PW, Mekonnen MM, Hoekstra AY. (2013) The water footprint of poultry, pork and beef: A comparative study in different countries and production systems. *Water Resources and Industry*; 1-2, 25-36. Doi.org/10.1016/j.wri.2013.03.001.

Goh TK, Zhang ZY, Chen AK, Reuveny S, Choolani M, Chan JK, Oh SK. (2013). Microcarrier culture for efficient expansion and osteogenic differentiation of human fetal mesenchymal stem cells. *Biores Open Access*, 2(2), 84-97. Doi: 10.1089/biores.2013.0001.

Grossi G, Goglio P, Vitali A, Williams AG (2019) Livestock and climate change: impact of livestock on climate and mitigation strategies. *Animal Frontiers*; 9(1), 69-76. Doi.org/10.1093/af/vfy034.

Hanga MP, Murasiewicz H, Pacek A, Nienow AW, Coopman K, Hewitt CJ. (2017) Expansion of bone marrow-derived human mesenchymal stem/stromal cells using a two-phase liquid/liquid system. *J. Chem. Technol. Biotechnol*; 92, 1577-1589. Doi: 10.1002/jctb.5279.

Heathman TRJ, Stolzing A, Fabian C, Rafiq QA, Coopman K, Nienow AW, Kara B, Hewitt CJ. (2015). Serum-free process development: improving the yield and consistency of human mesenchymal stromal cell production. *Cytotherapy*, 17(11), 1524-1535. doi: 10.1016/j.jcyt.2015.08.002.

Heathman TRJ, Rafiq QA, Chan AKC, Coopman K, Nienow AW, Kara B, Hewitt CJ (2016). Characterization of hMSC from multiple donors and the implications for large scale bioprocess development. *Biochem Eng J*; 108, 14-23. Doi.org/10.1016/j.bej.2015.06.018

Heathman TRJ, Nienow AW, Rafiq QA, Coopman K, Kara B, Hewitt CJ (2018). Agitation and aeration of stirred-bioreactors for the microcarrier culture of human mesenchymal stem cells and potential implications for large-scale bioprocess development. *Biochem. Eng. J.*, 136, 9–17. Doi.org/10.1016/j.bej.2018.04.011

Hewitt CJ, Lee K, Nienow AW, Thomas RJ, Smith M, Thomas CR. (2011). Expansion of human mesenchymal stem cells on microcarriers. *Biotechnol Lett*, 33(11), 2325-35. Doi: 10.1007/s10529-011-0695-4

Hill ABT, Bressan FF, Murphy BD, Gracia M J (2019). Applications of mesenchymal stem cell technology in bovine species. *Stem Cell Res. & Therapy*. 10, article number 44. Doi:10.1186/s13287-019-1145-9.

Kadim IT, Mahgoub O, Baqir S, Fave B, Purchas R (2015). Cultured meat from muscle stem cells: A review of challenges and prospects. *Journal of Integrative Agriculture*, 14(2), 222–233. Doi: 10.1016/S2095-3119(14)60881-9

Kuiper NJ, Sharma I (2015) A detailed quantitative outcome measure of glycosaminoglycans in human articular cartilage for cell therapy and tissue engineering strategies. *Osteoarthritis and cartilage*. 23(12), 2233-2241. doi.org/10.1016/j.joca.2015.07.011.

Lawson T, Kehoe DE, Schnitzel AC, Rapiejko PJ, Der KA, Philbrick K, Punreddy S, Rigby S, Smith R, Feng Q, Murrell JR, Rook MS (2017) Process development for expansion of human mesenchymal stromal cells in a 50 L single use stirred tank bioreactor. *Biochem Eng J*, 120, 49-62. Doi.org/10.1016/j.bej.2016.11.020.

Listrat A, Lebreton B, Louveau I, Astruc T, Bonnet M, Lefaucheur L, Brigitte Picard B and Jérôme Bugeon J, (2016) How Muscle Structure and Composition Influence Meat

and Flesh Quality, *The Scientific World Journal*; 2016, 3182746.
doi.org/10.1155/2016/3182746

Mattick CS, Landis AE, Allenby BR, Genovese NJ. (2015) Anticipatory Life Cycle Analysis of In Vitro Biomass Cultivation for Cultured Meat Production in the United States. *Environ Sci Technol.*; 49(19):11941-11949. doi: 10.1021/acs.est.5b01614.

Mouat MJ & Prince R. (2018) Cultured meat and cowless milk: on making markets for animal-free food, *Journal of Cultural Economy*, 11(4), 315-329.
Doi.org/10.1080/17530350.2018.1452277

Nienow AW, Coopman K, Heathman TRJ, Rafiq QA, Hewitt CJ. (2016a) Bioreactor engineering fundamentals for stem cell manufacturing. In “Stem Cell Manufacturing”, (Eds. Cabral J.M.S., de Silva C.L, Chase L. G., Diogo M. M.), Elsevier Science, Cambridge, USA; Chapter 3, pp 43 – 76. ISBN 978-0-444-63265-4,
<http://dx.doi.org/10.1016/B978-0-444-63265-4.00003-0>

Nienow AW, Hewitt CJ, Heathman TRJ, Glyn VAM, Fonte GN, Hanga MP, Coopman K, Rafiq QA (2016b) Agitation conditions for the culture and detachment of hMSCs from microcarriers in multiple bioreactor platforms. *Biochem. Eng. J.*, 108:24-29.
Doi.org/10.1016/j.bej.2015.08.003.

OECD-FAO Agricultural Outlook (2016-2025), OECD Publishing, Paris.
http://dx.doi.org/10.1787/agr_outlook-2016-en

Okamura LH, Cordero P, Palomino J, Parraguez VH, Torres CG, Peralta OA. (2018) Myogenic differentiation potential of mesenchymal stem cells derived from fetal bovine bone marrow. *Animal Biotechnol*; 29(1), 1-11. Doi: 10.1080/10495398.2016.12769

Rafiq QA, Brosnan KM, Coopman K, Nienow AW, Hewitt CJ. (2013). Culture of human mesenchymal stem cells on microcarriers in a 5 L stirred-tank bioreactor. *Biotechnol Lett*, 35(8), 1233-1245. Doi: 10.1007/s10529-013-1211-9.

Rafiq QA, Hanga MP, Heathman TRJ, Coopman K, Nienow AW, Williams DJ, Hewitt CJ. (2017). Process development of multipotent stromal cell microcarrier culture using an automated high-throughput microbioreactor. *Biotechnol Bioeng*. 114(10), 2253-2266. Doi: 10.1002/bit.26359.

Rafiq QA, Ruck S, Hanga MP, Heathman TJ, Coopman K, Nienow AW, Williams DJ, Hewitt CJ. (2018) Qualitative and quantitative demonstration of bead-to-bead transfer with bone marrow-derived human mesenchymal stem cells on microcarriers: utilising the phenomenon to improve culture performance. *Biochem. Eng. J.*; 135, 11-21. Doi.org/10.1016/j.bej.2017.11.005.

Salonen AO & Helne TT. (2012) Vegetarian Diets: A Way towards a Sustainable Society, *Journal of Sustainable Development*, 5(6). Doi:10.5539/jsd.v5n6p10

Schirmaier C, Jossen V, Kaiser SC, Jüngerkes F, Brill S, Safavi-Nab A, Siehoff A, van den Bos C, Eibl D, Eibl R. (2014). Scale-up of adipose tissue-derived mesenchymal stem cell production in stirred single-use bioreactors under low-serum conditions. *Engineering in Life Sciences*, 14(3), 292-303. Doi.org/10.1002/elsc.201300134

Schop D, Janssen FW, van Rijn LDS, Fernandes H, Bloem RM, de Bruijn JD, van Dijkhuizen-Radersma R (2009) Growth, metabolism and growth inhibitors of mesenchymal stem cells. *Tiss. Eng. Part A*; 15(8):1877-1886. doi: 10.1089/ten.tea.2008.0345.

Smetana S, Mathys A, Knoch A, Heinz V. (2015) Meat alternatives: life cycle assessment of most known meat substitutes. *Int J Life Cycle Assess.*; 20:1254-1267. doi.org/10.1007/s11367-015-0931-6

deSoure AM, Fernandes Platzgummer A, daSilva CL, Cabral JM. (2016) Scalable microcarrier-based manufacturing of mesenchymal stem/stromal cells. *Journal of Biotechnology*, 236:88-109. DOI: 10.1016/j.biotech.2016.08.007.

Stephens N, Di Silvio L, Dunsford I, Ellis M, Glencross A & Sexton A (2018) Bringing cultured meat to market: Technical, socio-political, and regulatory challenges in cellular agriculture, *Trends in Food Science & Technology*, 78, 155-166. Doi.org/10.1016/j.tifs.2018.04.010.

Tuomisto HL, de Mattos MJT (2011) Environmental impacts of cultured meat production. *Environ Sci Technol*; 45(14), 6117-6123. Doi.org/10.1021/es200130u.

Van der Plas A, Aarden EM, Feijen JH, de Boer AH, Wiltink A, Alblas MJ, de Leij L, Nijweide PJ (1994) Characteristics and properties of osteocytes in culture. *J Bone Miner Res*; 9(11), 1697-1704. Doi: 10.1002/jbmr.5650091105.

Van der Weele C and Tramper J (2014) Cultured meat: every village its own factory?; *Trends in Biotech*; 32(6):294-296. Doi: 10.1016/j.tibtech.2014.04.009.

Verbruggen S, Luining D, van Essen A, Post MJ (2017) Bovine myoblast cell production in a microcarriers-based system. *Cytotechnology*, 70, 503-512. Doi: 10.1007/s10616-017-0101-8

Wagner W, Horn P, Castoldi M, Diehlmann A, Bork S, Saffrich R, Benes V, Blake J, Pfister S, Eckstein V, Ho AD (2008) Replicative senescence of mesenchymal stem

cells: A continuous and organised process. *PLoS One*; 3(5), e2213. Doi: 10.1371/journal.pone.0002213.

Watt FM, Driskell RR (2010) The therapeutic potential of stem cells. *Philos Trans R Soc Lond B Biol Sci*; 365(1537), 155-163. DOI: 10.1098/rstb.2009.0149.

Table

Table 1. Growth kinetics for bAMSC expansion on microcarriers in spinner flasks when different feeding strategies were employed. Data presented as Mean \pm SD (n=5).

Medium exchange / Calculated parameter	80%	80/50%	65%	50%
Fold Increase	28.01 \pm 2.59	21.12 \pm 5.69	17.02 \pm 1.9	10.49 \pm 2.95
Specific growth rate (h ⁻¹)	0.0154 \pm 0.0004	0.0139 \pm 0.002	0.0131 \pm 0.001	0.0107 \pm 0.001
Doubling time (h)	45 \pm 1.28	50.31 \pm 6.57	52.95 \pm 2.03	65.15 \pm 7.15

Figures

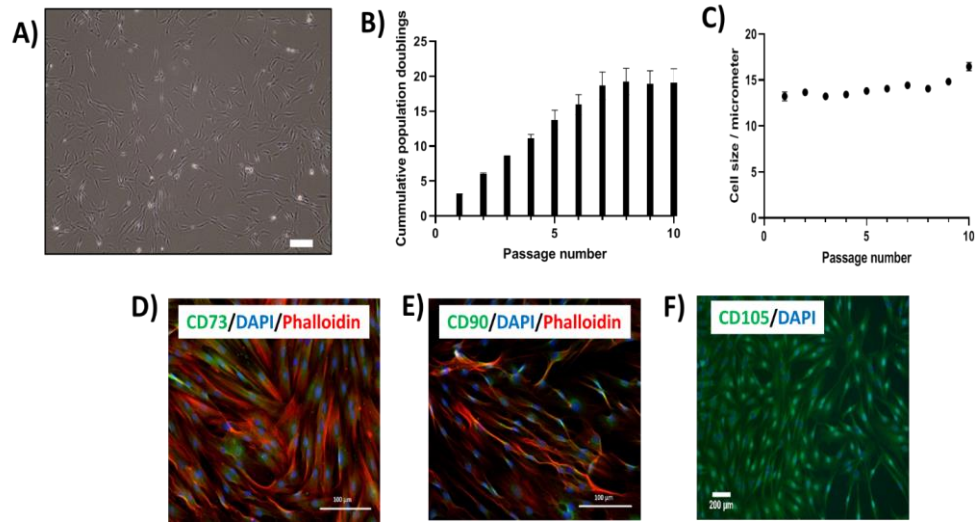


Figure 1. A) Bovine adipose-derived mesenchymal stem cell (bADSCs) morphology. Image taken at day 2 in culture. Scale bar represents 200 µm. B) Cumulative population doublings over 10 consecutive passages. C) Cell size (µm) over 10 consecutive passages. Data expressed as mean \pm SD, n=4. Immunofluorescence staining showing expression of D) CD73; E) CD90; F) CD105; Scale bars for D) and E) represent 100 µm, while for F) 200 µm.

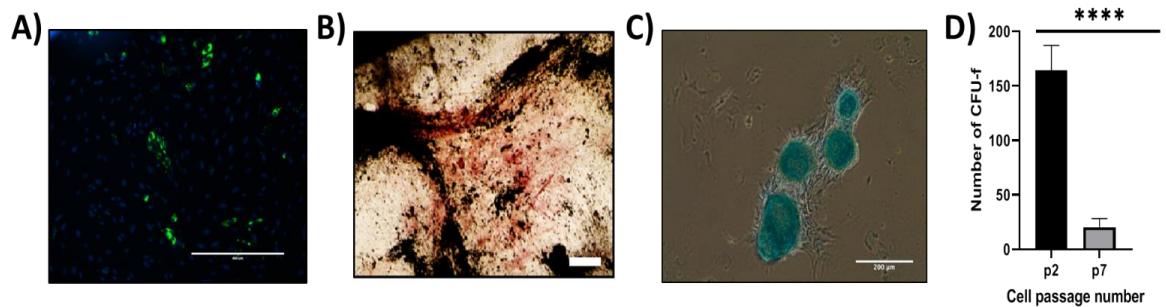


Figure 2. Pre-bioprocessing cell quality assessment. Differentiation staining of bASCs towards A) adipogenic (LipidTox staining), B) osteogenic (von Kossa stain) and C) chondrogenic (Alcian blue) lineages. Scale bar for adipogenic represents 400 µm. Scale bars for osteogenic and chondrogenic represent 200 µm. D) Clonogenic potential of bASCs at early (p2) and late (p7) passage numbers. Data expressed as mean \pm SD, n=5.

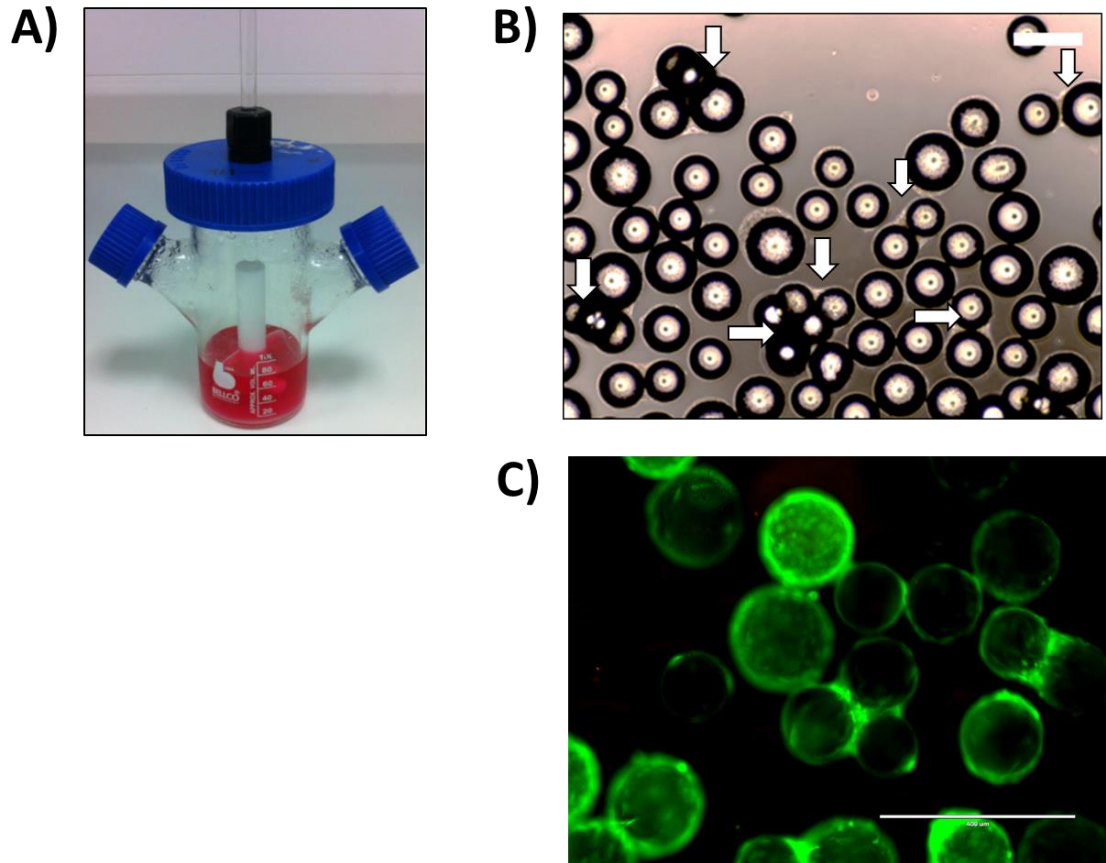


Figure 3. A) Spinner flask. B) Phase contrast image taken at day 5 in culture showing bASCs attached to microcarriers forming cell-microcarrier bridges. White arrows indicate cell bridging. Scale bar represents 200 μm . C) Live (green)/dead (red) staining of bASCs on microcarriers at day 5 in culture. Scale bar represents 400 μm .

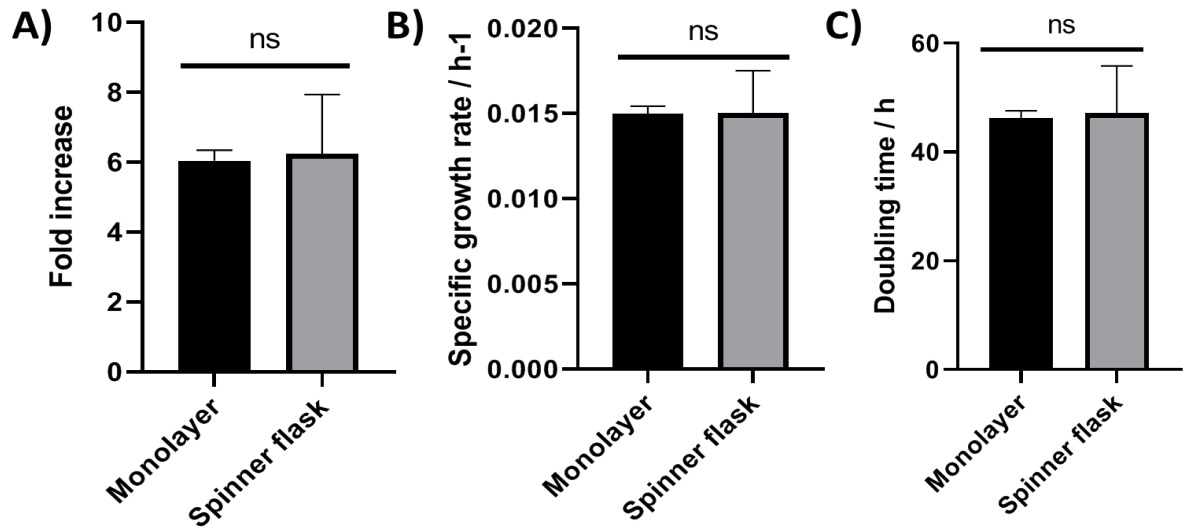


Figure 4. Comparison between monolayer and microcarrier culture in spinner flasks of bASCs at passage 3. A) Fold increase. B) Specific growth rate. C) Doubling time. Data shown as mean \pm SD; n=3. ns – not significant (unpaired t-tests).

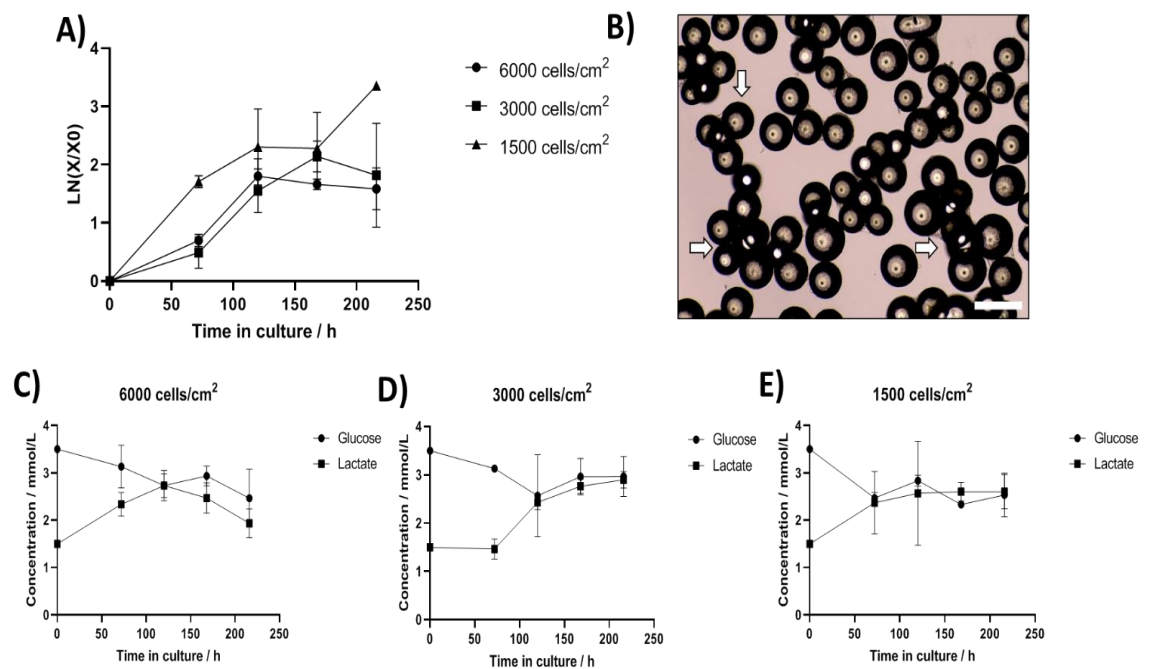


Figure 5. bASCs expansion in spinner flasks at different cell seeding densities. A) Specific growth at different cell seeding densities over 9 days in culture. B) Aggregation at day 5 as indicated by white arrows when using 6,000 cells/cm² as a seeding density. Scale bar represents 200 μ m. Glucose and lactate profiles for: C) 6,000 cells/cm²; D) 3,000 cells/cm²; E) 1,500 cells/cm². Data shown as mean \pm SD; n=3.

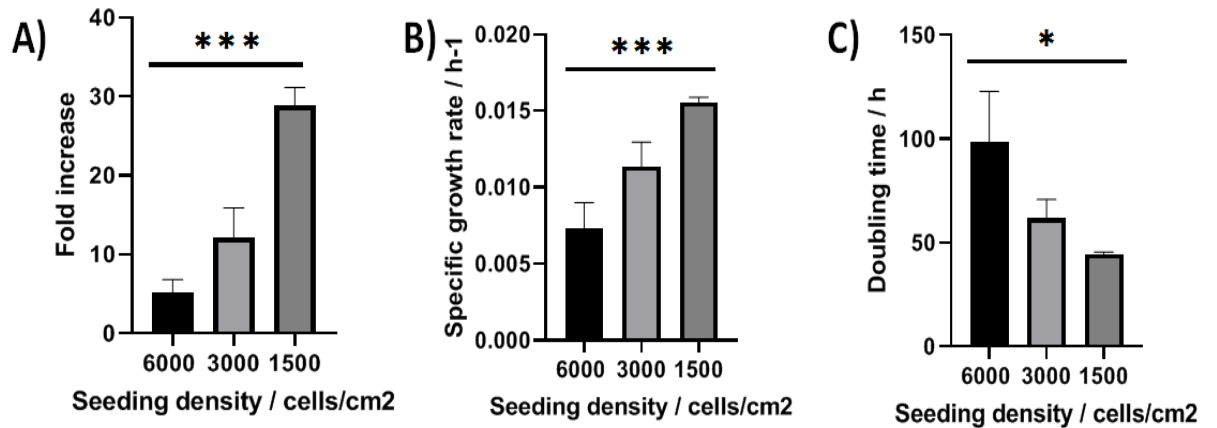


Figure 6. Growth kinetics comparison at different cell seeding densities. A) Fold increase; B) Specific growth rate; C) Doubling time. Data shown as mean \pm SD; n=3.

***p<0.0001; *p<0.05 (One way ANOVA).

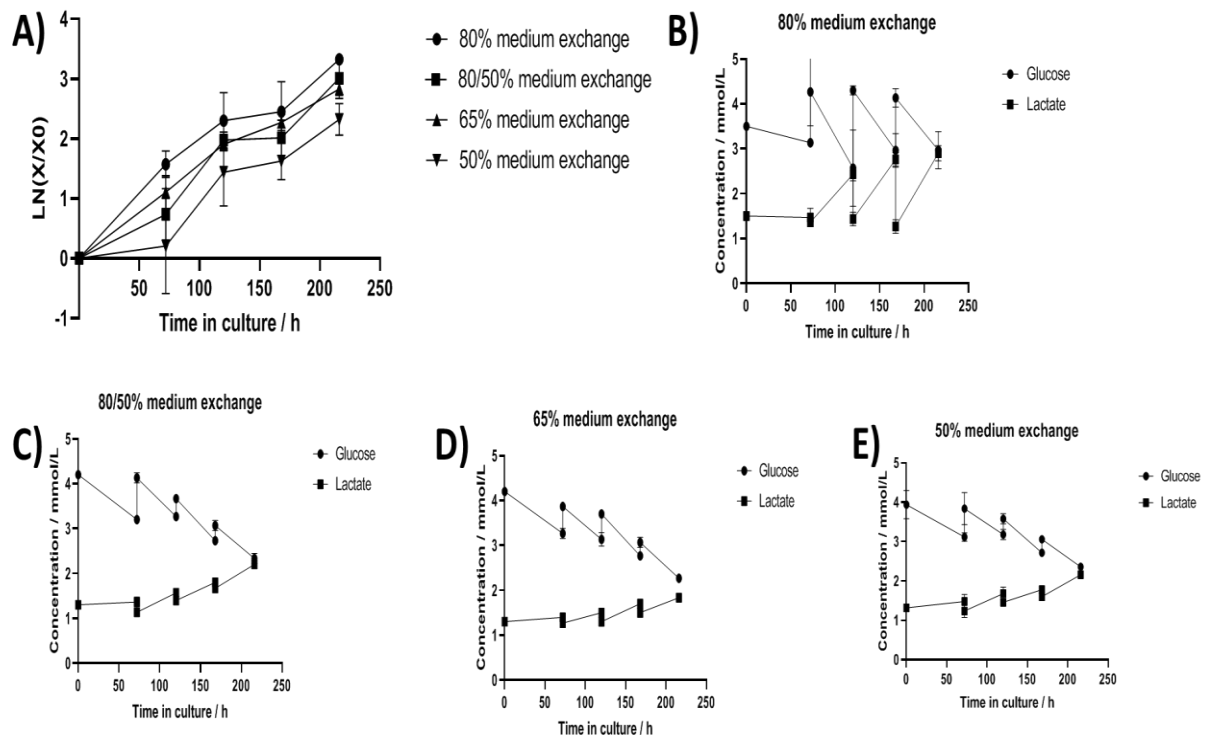


Figure 7. A) The effect of different feeding strategies on cell growth. Glucose and lactate profiles for different feeding strategies: B) 80% medium exchange; C) 80/50% medium exchange; D) 65% medium exchange; E) 50% medium exchange. Data expressed as mean \pm SD, n=5.

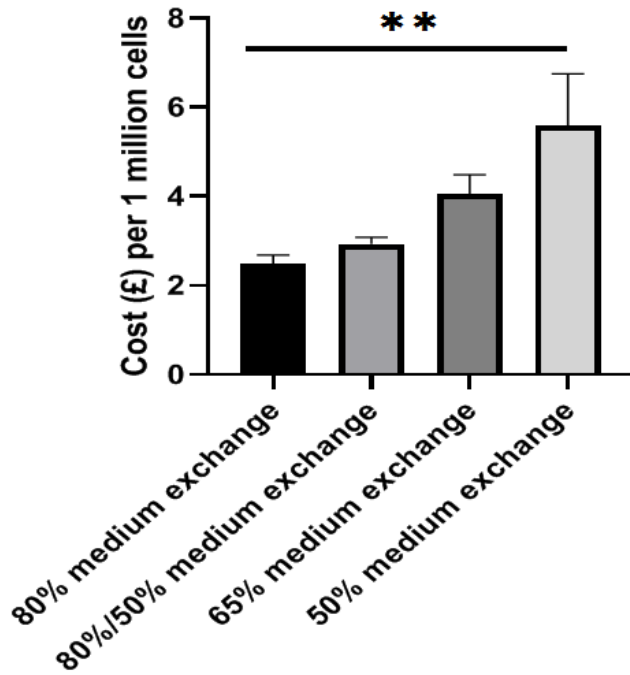


Figure 8. Cost (£) per million of cells produced when using different feeding strategies.

Data expressed as mean \pm SD, n=3.

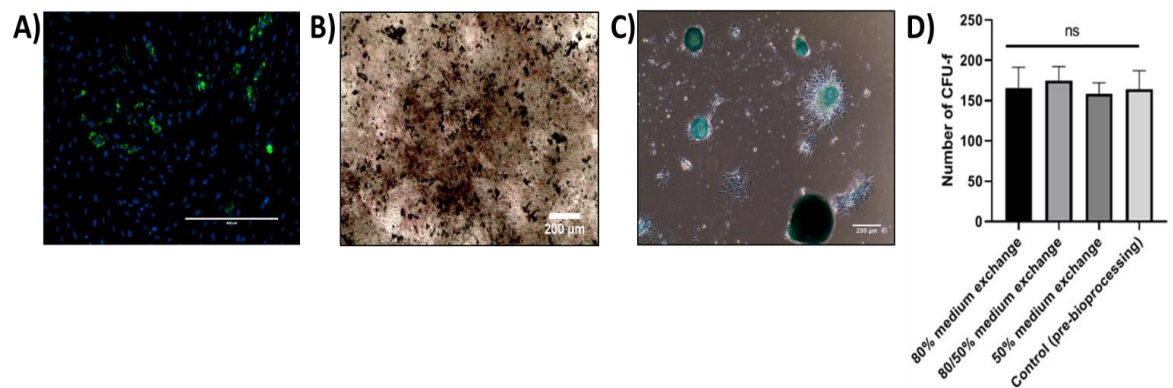


Figure 9. Post-bioprocessing cell quality assessment. Differentiation staining of bASCs towards A) adipogenic (LipidTox staining), B) osteogenic (von Kossa stain) and C) chondrogenic (Alcian blue) lineages. Scale bar for adipogenic represents 400 μ m. Scale bars for osteogenic and chondrogenic represent 200 μ m. D) Clonogenic potential of bASCs post-expansion when using different feeding strategies. Data expressed as mean \pm SD, n=5.